REPORT DOCUMENTATION PAGE

2

Form Approved OMB NO. 0704-0188

1. REPORT DATE (DD-MM-YYYY)	2. REPORT TYPE	3. DATES COVERED (From - To)
	New Reprint	-

4. TITLE AND SUBTITLE

Different Interfacial Behaviors of N- and C-Terminus Cysteine-Modified Cecropin P1 Chemically Immobilized onto Polymer Surface

5a. CONTRACT NUMBER

W911NF-11-1-0251

5b. GRANT NUMBER

5c. PROGRAM ELEMENT NUMBER

611103

6. AUTHORS

Xiaofeng Han, Joshua R. Uzarski, Charlene M. Mello, Zhan Chen

5d. PROJECT NUMBER

5e. TASK NUMBER

5f. WORK UNIT NUMBER

7. PERFORMING ORGANIZATION NAMES AND ADDRESSES

University of Michigan - Ann Arbor
3003 S. State St

Ann Arbor, MI 48109 -1274

8. PERFORMING ORGANIZATION REPORT NUMBER

9. SPONSORING/MONITORING AGENCY NAME(S) AND ADDRESS (ES)

U.S. Army Research Office
P.O. Box 12211
Research Triangle Park, NC 27709-2211

10. SPONSOR/MONITOR'S ACRONYM(S)

ARO

11. SPONSOR/MONITOR'S REPORT NUMBER(S)

59743-CH-MUR.35

12. DISTRIBUTION AVAILIBILITY STATEMENT

Approved for public release; distribution is unlimited.

13. SUPPLEMENTARY NOTES

The views, opinions and/or findings contained in this report are those of the author(s) and should not contrued as an official Department of the Army position, policy or decision, unless so designated by other documentation.

14. ABSTRACT

Sum frequency generation (SFG) vibrational spectroscopy and attenuated total reflectance-Fourier transform infrared spectroscopy (ATR-FTIR) were used to investigate the orientation of N-terminus cysteine-modified cecropin P1 (cCP1) at the polystyrene maleimide (PS-MA)/ peptide phosphate buffer solution interface. The cCP1 cysteine group reacts with the maleimide group on the PS-MA surface
to chemically immobilize cCP1. Previously, we found that the C-terminus cysteine-modified cecropin P1 (CP1c) molecules exhibit a multiple orientation distribution at the PS-MA/peptide phosphate buffer solution interface, due

15. SUBJECT TERMS

SFG, surface immobilization, peptides

16. SECURITY CLASSIFICATION OF:			17. LIMITATION OF ABSTRACT	15. NUMBER OF PAGES	19a. NAME OF RESPONSIBLE PERSON
a. REPORT	b. ABSTRACT	c. THIS PAGE			Zhan Chen
UU	UU	UU	UU		19b. TELEPHONE NUMBER: 734-615-4189

Report Title

Different Interfacial Behaviors of N- and C-Terminus Cysteine-Modified Cecropin P1 Chemically Immobilized onto Polymer Surface

ABSTRACT

Sum frequency generation (SFG) vibrational spectroscopy and attenuated total reflectance-Fourier transform infrared spectroscopy (ATR-FTIR) were used to investigate the orientation of N-terminus cysteine-modified cecropin P1 (cCP1) at the polystyrene maleimide (PS-MA)/ peptide phosphate buffer solution interface. The cCP1 cysteine group reacts with the maleimide group on the PS-MA surface
to chemically immobilize cCP1. Previously, we found that the C-terminus cysteine-modified cecropin P1 (CP1c) molecules exhibit a multiple-orientation distribution at the PS-MA/peptide phosphate buffer solution interface, due to simultaneous physical adsorption and chemical immobilization of CP1c on the PS-MA surface. Differently, in this research, it was found that the interfacial orientation of cCP1 molecules varied from a horizontal orientation to the "tilting" orientation to the "standing up" orientation and then to the "multiple-orientation" distribution as the peptide concentration increased from 0.19 to 3.74 ?M. This research shows the different interaction mechanisms between CP1c and PS-MA and between cCP1 and PS-MA.

REPORT DOCUMENTATION PAGE (SF298)
(Continuation Sheet)

Continuation for Block 13

ARO Report Number 59743.35-CH-MUR
Different Interfacial Behaviors of N- and C-Term...

Block 13: Supplementary Note

Approved for public release; distribution is unlimited.

Langmuir

Article

pubs.acs.org/Langmuir

Different Interfacial Behaviors of N- and C-Terminus Cysteine-Modified Cecropin P1 Chemically Immobilized onto Polymer Surface

Xiaofeng Han,[†] Joshua R. Uzarski,[‡] Charlene M. Mello,*[,‡] and Zhan Chen*[,†]

[†]Department of Chemistry, University of Michigan, Ann Arbor, Michigan 48109, United States

[‡]Bioscience and Technology Team, U.S. Army Natick Soldier Research, Development, & Engineering Center (NSRDEC), Natick, Massachusetts 01760-5020, United States

ABSTRACT: Sum frequency generation (SFG) vibrational spectroscopy and attenuated total reflectance-Fourier transform infrared spectroscopy (ATR-FTIR) were used to investigate the orientation of N-terminus cysteine-modified cecropin P1 (cCP1) at the polystyrene maleimide (PS-MA)/peptide phosphate buffer solution interface. The cCP1 cysteine group reacts with the maleimide group on the PS-MA surface to chemically immobilize cCP1. Previously, we found that the C-terminus cysteine-modified cecropin P1 (CP1c) molecules exhibit a multiple-orientation distribution at the PS-MA/peptide phosphate buffer solution interface, due to simultaneous physical adsorption and chemical immobilization of CP1c on the PS-MA surface. Differently, in this research, it was found that the interfacial orientation of cCP1 molecules varied from a horizontal orientation to the "tilting" orientation to the "standing up" orientation and then to the "multiple-orientation" distribution as the peptide concentration increased from 0.19 to 3.74 μM. This research shows the different interaction mechanisms between CP1c and PS-MA and between cCP1 and PS-MA.

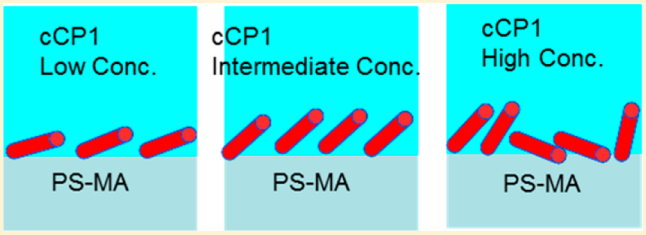

1. INTRODUCTION

Biosensors have been widely used to detect pathogens.[1−13] A fundamental and key factor for such a device design is the biological recognition element interacting with the target pathogen. These elements can be composed of DNA segments,[6,7] peptides,[10−17] or proteins (e.g., enzymes or antibodies).[18,19] Protein- and peptide-based biological recognition elements can be adsorbed, trapped, or immobilized on a surface. Biosensor performance (e.g., sensitivity, selectivity, detection limit, precision, accuracy, reproducibility, working life, and shelf life) is greatly affected by the structures and orientations of the interfacial sensing biological molecules.[20−22]For example, in the case of proteins and peptides, they must be properly oriented so that the binding domains are accessible while preserving their sensor functions. Many current pathogen detection systems use antibodies, which exhibit specificity for pathogenic bacteria but lack the stability needed for detection in harsh environments and exhibit insufficient control of immobilization orientation.[14] Recently, naturally occurring antimicrobial peptides (AMPs) have been studied as an alternative with a broad range of activity and binding affinity toward microorganisms.[10−16] For example, chemically immobilized cecropin P1, cecropin A, cecropin B, and other antimicrobial peptides have demonstrated promise for capturing and sensing the bacterial pathogen *E. coli* O157:H7.[10,13,15,16]

Numerous surface immobilization methods have been used to improve the performance of protein- and peptide-based biosensors, but the effect of molecular structure and orientation has not yet been elucidated in detail. This is largely due to the lack of appropriate analytical techniques. Recently, sum frequency generation (SFG) vibrational spectroscopy has been applied to investigate peptides and proteins at solid/liquid interfaces in situ.[23−40] SFG is a second-order nonlinear optical spectroscopic technique with submonolayer surface sensitivity. In our lab we successfully developed systematic methodologies to determine interfacial orientations of various secondary structures such as the α-helix, 3−10 helix, β-sheet, and complex proteins such as G proteins using polarized SFG spectra.[31−33,39] We applied these methods to deduce interfacial orientations of a variety of peptides and proteins at solid/water interfaces.[34,35,37−40] In particular, we examined the orientation of physically adsorbed and chemically immobilized α-helical cecropin P1 on polymer surfaces.[35,38]To promote chemical immobilization, the C-termini of the cecropin P1 were modified with a cysteine residue (CP1c), which forms covalent thioether bonds with polystyrene maleimide (PS-MA). We found that upon physical adsorption onto a polystyrene (PS) surface CP1c molecules adopt a multiple-orientation distribution which could not be described by a delta or Gaussian distribution.[35] CP1c molecules at the PS-MA/peptide solution interface also exhibited a multiple-orientation distribution even at very low peptides concentration; however, after washing off the physisorbed CP1c molecules, the chemically immobilized CP1c molecules at the PS-MA/peptide solution interface exhibited an orientation angle of 35° versus the surface normal.

Received: May 23, 2013
Revised: July 26, 2013
Published: August 6, 2013

This work demonstrated that the physically adsorbed and chemically immobilized CP1c molecules adopt different orientations at the polymer/peptide solution interface.

Mello et al. investigated the interactions between CP1c and pathogenic *E. coli*[13] and showed that when CP1c molecules were deposited on surfaces using different methods, the activities of the surface-immobilized CP1 molecules varied. For example, CP1 molecules physically adsorbed and chemically immobilized via the C-terminus exhibited very different killing efficiencies against *E. coli*. Furthermore, the overall binding proclivity of cecropin P1 to lipopolysaccharide molecules isolated from the outer membranes of different *E. coli* serotypes depends on the orientation of the immobilized peptide, with the C-terminal peptide showing higher binding than the N-terminal one.[17] Such observations may be partially interpreted, using our SFG results, to mean that CP1c molecules adopt different orientations/orientation distributions when different surface immobilization/adsorption methods are used. Such binding differences may also be related to the position of the charged residues in the immobilized cecropin P1 relative to the distance from the surface.

In this research, we will investigate the interfacial behavior of N-terminal cysteine-modified cecropin P1 (cCP1). We will compare such results to those previously obtained from CP1c molecules immobilized on the surface and will be able to use the different structures of cecropin P1 immobilized via different termini to interpret their different activities. We believe that this is the first attempt to elucidate the structure−function relationship of the same peptide immobilized via different termini. When cCP1 molecules contact a PS-MA surface, the N-terminal cysteine will react to form covalent thioether bonds with the maleimide group, chemically immobilizing the peptide onto the PS-MA surface. Different from the CP1c peptides, SFG results indicate that the cCP1 molecules at the PS-MA/peptide solution interface exhibit a single orientation distribution at low peptide concentrations ($\leq$0.75 μM); the orientation angle is dependent on the peptide solution concentration. At higher peptide concentrations ($\geq$1.23 μM), the cCP1 molecules adopt a multiple-orientation distribution. ATR-FTIR experiments were performed to measure the relative cCP1 adsorption amount on the PS-MA surface.

2. EXPERIMENTAL SECTION

2.1. Materials and Sample Preparation. All of the chemicals were used as received. (4-Maleimidobutyramidomethyl) polystyrene (PS-MA), potassium phosphate (monobasic and dibasic) solution (1 M), tris(2-carboxyethyl)phosphine hydrochloride (TCEP) solution (0.5 M), dichloromethane, toluene, and deuterated water (D_2O) were all purchased from Aldrich (Milwaukee, WI). The N-terminus cysteine-modified CP1 (cCP1, H_2N-CSWLSKTAKKLENSAKKRISEGIAIAIQGGPR-OH, MW = 3442) was ordered from New England Peptide (Gardner, MA). EDTA was obtained from Fisher Biotech. Right-angle CaF_2 prisms were purchased from Altos (Bozeman, MT) and thoroughly cleaned using a multistep procedure as described in our previous publication.[38]

PS-MA films were prepared by directly depositing 0.01% PS-MA/dichloromethane solution onto CaF_2 prisms. Polymer films were kept at room temperature for 24 h prior to performing SFG experiments. A 50 mM phosphate buffer with a pH of 7.2 was prepared by mixing monobasic potassium phosphate solution (1 M), dibasic potassium phosphate solution (1 M), and DI water (purified by a Millipore system). A specific amount of cCP1 was dissolved into 5 mM phosphate buffer with reducing agent TCEP and EDTA. TCEP was added to prevent disulfide bond formation among individual peptide molecules, which ensures that a thiol moiety was present in a cCP1 molecule. The thiol moiety in the cysteine residue has a strong affinity for the maleimide moieties, which promotes covalent immobilization of the peptide to the PS-MA surface. EDTA was added as a chelating agent to oxidize any metals present in the buffer that may cause formation of unwanted disulfide bonds. The thiol moiety in the cysteine residue can chemically react with a maleimide group on the surface, which promotes covalent immobilization of cCP1 onto the PS-MA surface (Figure 1).

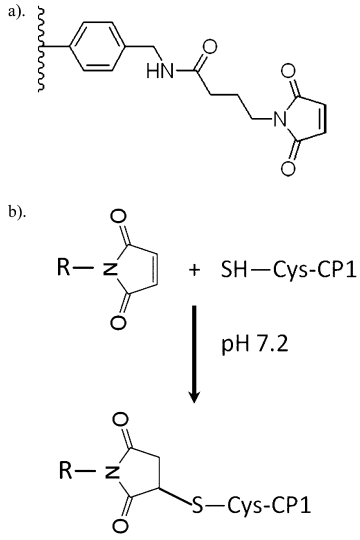

Figure 1. (a) (4-Maleimidobutyramidomethyl) polystyrene. (b) Schematic showing cysteine-modified CP1 covalently tethered to a maleimide group.

2.2. SFG Measurements. Details regarding SFG theories and equipment have been reported previously[41−59] and will not be repeated here. In our SFG experiments, right angle CaF_2 prisms were used to realize the near total reflection geometry.[23] In this geometry, the incident angles for the input visible and IR beams are 57° and 60° with respect to the Z axis in the lab coordinate system (Z axis is perpendicular to the surface).[23] All of the SFG experiments were carried out at room temperature (23 °C). SFG spectra with different polarization combinations including ssp (s-polarized SF output, s-polarized visible input, and p-polarized infrared input) and ppp were collected using the near total internal reflection geometry. When a near total reflection geometry is adopted in the SFG experiment, ppp signal probes χ_{zzz}. More details of the SFG data analysis can be found in the Supporting Information of ref 35.

2.3. ATR-FTIR Experiments. A Nicolet 6700 FTIR spectrometer was used to collect ATR-FTIR spectra with a standard 45° ZnSe ATR cell. ZnSe crystal was cleaned using the same procedure as the CaF_2 prisms. PS-MA films were prepared by directly depositing the PS-MA solution onto the ATR crystal (ZnSe). Polymer films were equilibrated with D_2O buffer solution prior to collection of a background spectrum of the PS-MA polymer film/D_2O buffer solution interface. D_2O buffer was replaced with the peptide solution (in D_2O buffer) and equilibrated for at least 1 h to allow for peptide adsorption to reach equilibrium at the interface. The ATR-FTIR spectrum was then collected from the PS-MA/peptide D_2O buffer solution interface. Finally, the amide I and amide II signals of adsorbed/immobilized peptide molecules on the PS-MA surface were obtained by subtracting the background spectrum of the polymer film/D_2O buffer solution interface from the later collected spectrum. All ATR-FTIR spectra collected in this work were averages of 128 scans with a 2 cm^{-1} resolution.

3. RESULTS AND DISCUSSIONS

3.1. Different Behaviors of cCP1 and CP1c on PS-MA/Peptide Solution Interfaces. Our previous SFG studies on

CP1c molecules indicated that when phosphate buffer was used as the solvent the CP1c molecules at the PS-MA/CP1c buffer solution interface adopted a multiple-orientation distribution.[38] The χ_{ppp}/χ_{ssp} signal strength ratio was beyond the possible range described by a delta or Gaussian distribution. Therefore, the distribution possibly contained several orientations, like the melittin case we studied previously.[31] However, after washing the interface several times using the buffer solution, the CP1c orientation could be described by a delta or Gaussian distribution.[38] This is because the physisorbed CP1c molecules can be washed away from the interface, leaving only chemically immobilized CP1c molecules. In this work, cCP1 molecules at the PS-MA/cCP1 buffer solution interfaces have been studied by SFG and ATR-FTIR. Different from the CP1c behavior at the PS-MA/CP1c solution interfaces, the orientations of cCP1 molecules at the PS-MA/cCP1 solution interface could be described by a delta or Gaussian distribution at low peptide concentrations, which will be presented in more detail below. For some experiments, the peptide solution in contact with the PS-MA was replaced with buffer solution several times to wash away the loosely associated peptides at the PS-MA/peptide solution interface. In this case, chemically immobilized cCP1 molecules on the PS-MA surface should be the only contributor to the SFG signal, which exhibits a similar orientation angle.

SFG ssp and ppp spectra were collected from the interface between the PS-MA surface and the peptide buffer solution. For an α-helix, we have shown previously that the χ_{ppp}/χ_{ssp} signal strength ratio (taken after fitting the ppp and ssp spectra) can be used to determine its orientation.[32,38] The relationship between the χ_{ppp}/χ_{ssp} signal strength ratio and the CP1 orientation described by a delta or Gaussian distribution is shown in Figure 2. The orientation angle θ is the angle between the α-helix principal axis and the surface normal.

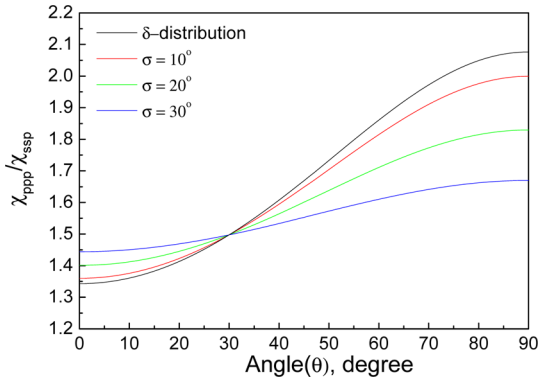

Figure 2. Relations between the SFG susceptibility tensor component ratio and the α-helix orientation angle with different orientation distributions (assuming Gaussian distributions).

3.2. Peptide Concentration Effect on cCP1 Orientation at the PS-MA/Peptide Solution Interface. *3.2.1. Low Peptide Concentration.* To better understand the orientation of cCP1 at the PS-MA/peptide solution interface, SFG spectra were collected from the cCP1 molecules at the PS-MA/peptide solution interface using cCP1 buffer solutions at different concentrations: 0.19, 0.28, 0.37, and 0.75 μM, as shown in Figure 3. All detected SFG spectra are dominated by a single peak centered at ~1650 cm^{-1}, showing that cCP1 molecules adopted an α-helical conformation at the PS-MA/peptide solution interface, which is similar to previous results from the CP1c molecules.[35,38] For 0.19 μM cCP1 solution, the fitted χ_{ppp}/χ_{ssp} signal strength ratio is about 2.2, as shown in Figure 3a. From the relationship between the χ_{ppp}/χ_{ssp} signal strength ratio and the α-helix orientation, we can see that cCP1 molecules more or less adopt a horizontal orientation at the interface. The SFG signals are quite weak for an accurate angle determination, perhaps due to the low surface coverage (because of the low concentration) of cCP1 molecules as well as the horizontal interfacial orientation of cCP1 molecules. In this case, because of the low surface coverage of cCP1 molecules, there is adequate available surface area to accommodate a horizontal cCP1 orientation. The low peptide surface coverage can be confirmed by later ATR-FTIR experimental data.

When the concentration of the cCP1 buffer solution increased, the cCP1 molecules at the PS-MA/peptide solution interface changed orientation. SFG spectra collected from the PS-MA/peptide solution interface when the cCP1 concentration was increased to 0.28 μM are shown in Figure 3b. The fitted χ_{ppp}/χ_{ssp} signal strength ratio leads to an orientation angle of 45° versus the surface normal. Compared to the 0.19 μM case above, when the concentration increased, more cCP1 molecules diffused to the interface and immobilized onto the PS-MA surface. Therefore, each molecule likely occupies a smaller surface area and tilt to accommodate the increased peptide density.

The interfacial cCP1 orientation could still be described by a single delta function when the peptide solution concentration was increased to 0.28 μM. It can be speculated that when more concentrated cCP1 solutions are used in the experiment, interfacial cCP1 molecules will adopt more than one orientation because more peptide molecules can be physisorbed or loosely associated at the interface, creating a multiple-orientation distribution.

We continued to increase the cCP1 buffer solution concentration to 0.37 μM. SFG spectra were collected from the PS-MA/peptide solution interface and are shown in Figure 3c. According to the fitted χ_{ppp}/χ_{ssp} signal strength ratio, the cCP1 average orientation was determined to be 15° versus the surface normal. When the peptide concentration reached 0.37 μM, the cCP1 molecules at the PS-MA/peptide solution interface are likely approaching saturation and therefore produce a tightly packed monolayer which adopt a more vertical orientation. Compared to the above two concentrations of 0.19 and 0.28 μM, more cCP1 molecules were adsorbed to the PS-MA surface, which can be confirmed by the ATR-FTIR results presented below. The measurement of 15° assumes that all molecules adopt the same orientation. Even though the cCP1 molecules were chemically immobilized at the PS-MA/peptide solution interface, we believe that these cCP1 molecules must have reached a dynamic equilibrium with those in the peptide solution. We hypothesized that if we removed the cCP1 molecules from the peptide solution, e.g., replaced the peptide solution with buffer, some of the immobilized cCP1 molecules would return to the liquid phase and a new equilibrium might be established. This was confirmed by replacing the peptide solution with buffer several times. SFG spectra were then collected from the PS-MA/buffer interface using the ssp and ppp polarization combinations (Figure 3e). The spectral intensities greatly decreased, and the fitted χ_{ppp}/χ_{ssp} signal strength ratio indicated that the cCP1 orientation was around 48°. It could be seen that when some of the molecules desorbed from the PS-MA surface, each cCP1

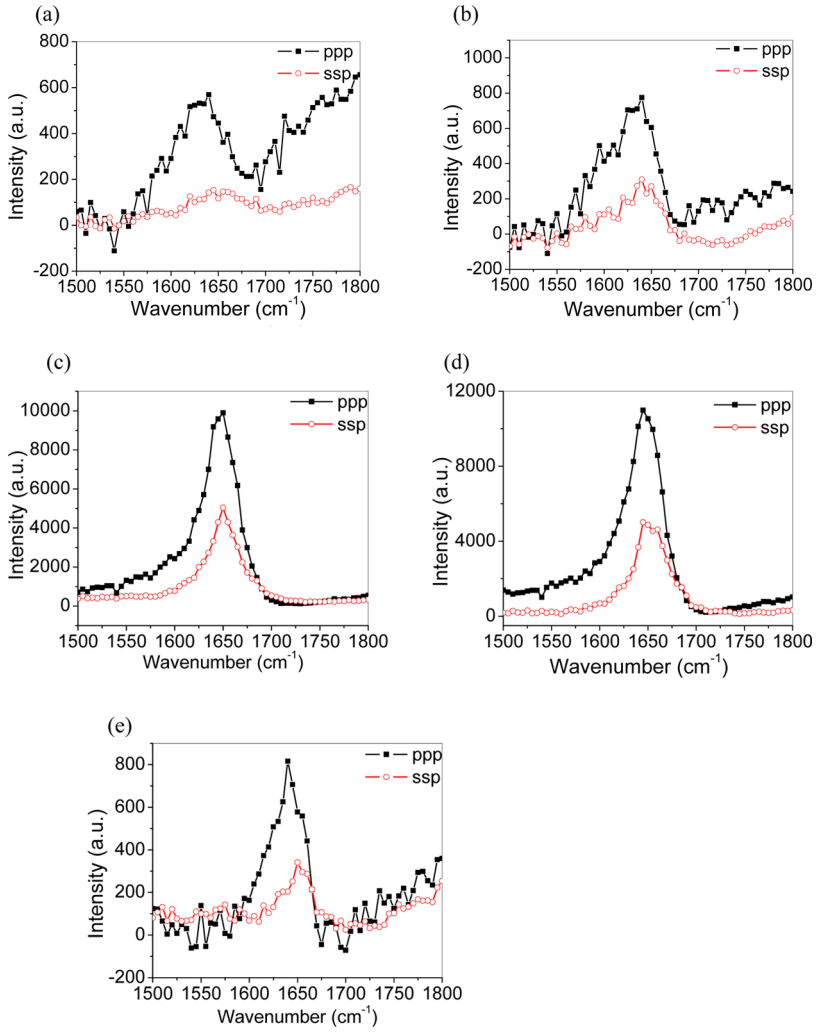

Figure 3. SFG spectra collected from cCP1 molecules at the PS-MA/peptide solution interface with different cCP1 PB concentrations: (a) 0.19, (b) 0.28, (c) 0.37, and (d) 0.75 μM. (e) SFG spectra collected from the cCP1 molecules at the PS-MA/PBS interface after the PS-MA surface is in contact with cCP1 PB solution with a concentration of 0.37 μM; then the cCP1 PB solution was washed by new PB solutions.

molecule had more space and thus could tilt more. It is possible that the optimal orientation for the immobilized cCP1 molecules on the PS-MA surface is around 50°, which is not very different from the previously tested C-terminus-modified CP1c molecules which were chemically immobilized on a PS-MA surface and washed with phosphate buffer (35°).

The cCP1 concentration was increased to 0.75 μM, and ssp and ppp SFG spectra were again recorded to deduce the peptide orientation at the PS-MA interface. In Figure 3d, the fitted χ_{ppp}/χ_{ssp} shows that the peptide orientation is approximately 10°. Despite a 2-fold increase in peptide solution concentration, the orientation difference between 0.75 and 0.37 μM cCP1 was small (10° vs 15°, respectively).

3.2.2. High Peptide Concentration. We then increased the cCP1 buffer solution concentration to 1.12, 1.50, and 3.74 μM and collected SFG ssp and ppp spectra from the cCP1 molecules at the PS-MA/peptide solution interfaces. These are displayed in Figures 4a, 4b, and 4c, respectively. At 1.12, 1.50, and 3.74 μM, the fitted χ_{ppp}/χ_{ssp} ratios were 1.29, 1.22, and 1.24. For all cases the ratio was similar and beyond the possible range for a delta or Gaussian distribution, indicating that the cCP1 molecules adopted a multiple-orientation distribution for these three cases. For the three concentrations, the SFG signal strength did not change substantially, similar to the CP1c case.[38]

After SFG spectra were collected from the interface between PS-MA and cCP1 solution with a concentration of 1.50 μM, the CP1 solution was replaced by buffer to wash the interface twice. SFG spectra were then collected from the PS-MA (with cCP1)/buffer interface, and the resulting data is shown in Figure 4d. The two-stage wash should remove the physisorbed cCP1 molecules, thereby allowing the remaining chemically immobilized cCP1 molecules to reach a new dynamic equilibrium. This was indeed the case as the fitted χ_{ppp}/χ_{ssp} ratio leads to a single cCP1 orientation angle of approximately 50°, which agrees with the results of the 0.19 μM cCP1 solution. The result of the higher peptide concentration after washing again shows the optimal orientation of chemically immobilized cCP1 is approximately 50° from the surface normal as shown in Table 1.

3.3. Relative Peptide Absorption Quantified by ATR-FTIR. SFG results showed that the χ_{ppp}/χ_{ssp} ratios measured from the SFG amide I spectra detected from cCP1 molecules at the PS-MA/cCP1 buffer solution interface changed as a function of peptide solution concentration. This suggests that the cCP1 peptide molecules changed orientations when the

dx.doi.org/10.1021/la401818k | *Langmuir* 2013, 29, 11705−11712

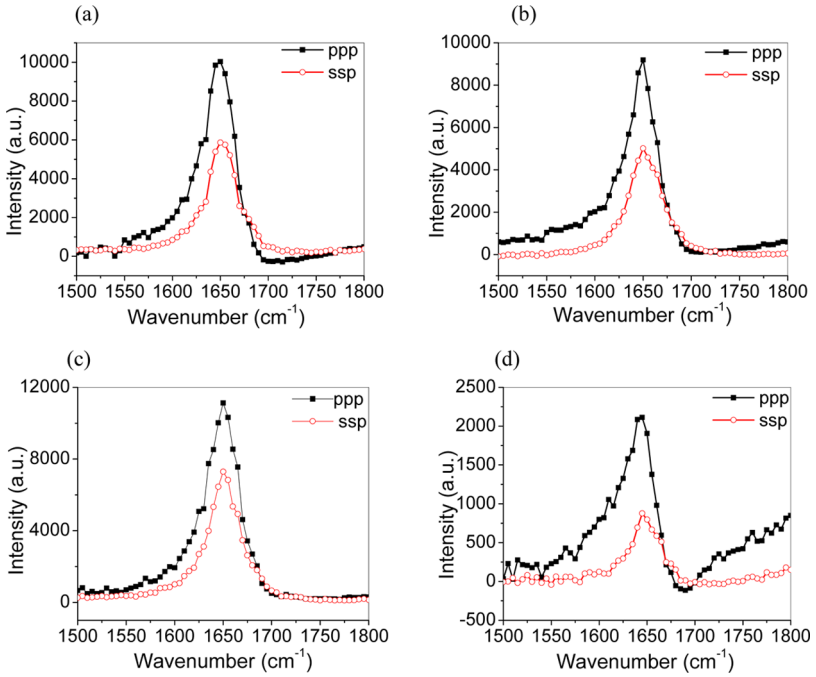

Figure 4. SFG spectra collected from cCP1 molecules at the PS-MA/peptide solution interface with different cCP1 PB concentrations: (a) 1.12, (b) 1.50, and (c) 3.74 μM. (d) SFG spectra collected from the cCP1 molecules at the PS-MA/PBS interface after the PS-MA surface is in contact with cCP1 PBS solution with a concentration of 1.50 μM; then the cCP1 PB solution was replaced by new PB solutions twice.

Table 1. Orientation Angle Deduced for N-Terminus Cysteine-Modified Cecropin P1 at PS-MA/Liquid Interfaces with Different Peptide Solution Concentrations

peptide concentration (μM)	0.19	0.28	0.37	0.75	1.12	1.50	3.74
tilt angle (deg) vs surface normal	lying down	50	15	10	multiple orientations	multiple orientations	multiple orientations
tilt angle (deg) vs surface normal after washing (replace the peptide solution with PBS for several times)			48	51	54	50	47

peptide concentration was varied. As discussed, the peptide orientation change might be due to the fact that more peptide molecules could adsorb or immobilize on the PS-MA surface at higher peptide concentrations. Differently, such measured χ_{ppp}/χ_{ssp} ratios remained more or less the same at higher peptide concentrations (when the solution concentration was at or higher than ~1.12 μM). To further demonstrate that the adsorption amount may be varied at different peptide concentrations, ATR-FTIR was applied to measure the relative adsorption amount of cCP1 molecules at interfaces.

Figure 5a shows the ATR-FTIR spectra of cCP1 molecules adsorbed to the PS-MA surfaces at different peptide solution concentrations, varying from 0.19 to 7.5 μM. To avoid spectral confusion between the H_2O bending signal and the peptide amide I signal, peptide D_2O buffer solution was used in the experiment. Use of D_2O in the peptide solution shifts the amide I peak center to slightly lower than 1650 cm^{-1}, showing that the signal is still dominated by the contribution from the α-helical component. With the peptide concentration change, no substantial ATR-FTIR spectral feature change was observed in the amide I frequency range, as shown in Figure 5a. This suggests that adsorbed cCP1 molecules at the PS-MA/peptide D_2O buffer solution interface adopt similar secondary structures (dominated by α-helix) at different peptide solution concentrations.

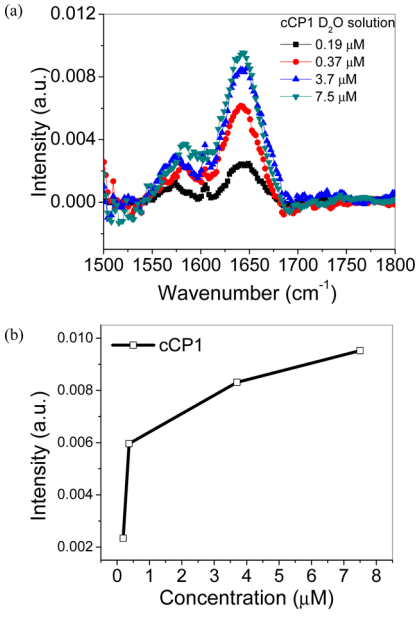

Figure 5. (a) ATR-FTIR spectra detected from the PS-MA/cCP1 buffer solution interface with different peptide solution concentrations. (b) ATR-FTIR signal intensities of the 1645 cm^{-1} peak at different peptide concentrations for cCP1.

dx.doi.org/10.1021/la401818k | *Langmuir* 2013, 29, 11705−11712

Using ATR/FTIR, we can then deduce the relative adsorption amount in a semiquantitative fashion of cCP1 at the PS-MA/peptide solution interface. Since ATR-FTIR is linear spectroscopy, the adsorption amount should be linearly related to the ATR-FTIR signal intensity. Figure 5b shows that the adsorption amount of cCP1 at the interface when the peptide concentration is 0.37 μM is about three times that at the interface when the peptide solution is 0.19 μM. This can be correlated to the SFG spectral intensity difference detected from these two cases. If we compare the SFG signal intensities observed in the ssp spectra, the intensity detected from the interfacial cCP1 at the peptide concentration of 0.37 μM is about 20 times compared to that detected at the peptide concentration of 0.19 μM. The adsorption amount difference observed by ATR-FTIR is responsible for a factor of 10 difference (SFG intensity is proportional to the square of adsorption amount), and the different orientations may lead to another factor of 2 (the lying-down orientation generates weaker SFG amide I signal from the α-helical structure). The weak SFG signal from the 0.19 μM case prohibits us to perform a quantitative analysis. However, we can see that the ATR-FTIR results can be correlated to SFG data in a semi-quantitative fashion.

Figure 5b also shows that the adsorbed amount of cCP1 at the interface when the peptide concentration is 3.7 μM is about 1.3 times of that at the peptide solution of 0.37 μM. The will lead to 1.3 × 1.3 = 1.7 times of the SFG amide I spectral intensity difference detected from these two cases. If we compare the SFG signal intensities observed in the ssp spectra, the one detected from the interfacial cCP1 at the peptide concentration of 3.7 μM is about 1.5 times compared to that detected at the peptide concentration of 0.37 μM. The slight difference between 1.5 and 1.7 might be due to the intensity dependence on the peptide orientation, which is difficult to quantify here. Nevertheless, here again we believe that the ATR-FTIR results are well correlated to the SFG data.

3.4. Further Discussion. It is important to note that after replacing the peptide solution with the buffer, the cCP1 molecules at the interface changed their orientations. For the 0.37 μM solution, the orientation changed from ~15° versus the surface normal to approximately ~50° versus the surface normal. For the 1.50 μM solution, the orientation of interfacial cCP1 molecules changed from a multiple-orientation distribution to a single orientation with approximately a 50° orientation angle versus the surface normal. It is also interesting to see that the final orientation of cCP1 molecules at the PS-MA/buffer interface is the same when the initial concentrations and interfacial orientations are different. It is reasonable for the two orientations to be similar since they are both measured from cCP1 molecules at the PS-MA/PB interface; this seems to be the preferential orientation. This orientation is also similar to that measured from the cCP1 molecules at the PS-MA/peptide solution interface with a peptide concentration of 0.28 μM.

When we investigated the CP1c molecules previously (C-terminus is cysteine modified), we found that a multiple-orientation distribution of CP1c was observed on the PS-MA surface regardless of the peptide concentrations, showing that both physical adsorption and chemical immobilization occurred.[35,38] Differently, here when cCP1 is used (N-terminus is cysteine modified), at low peptide concentrations, a single orientation of cCP1 was deduced at the interface. This study indicates clearly that the CP1c and cCP1 molecules interact with the PS-MA surface differently. Figure 6 shows a schematic

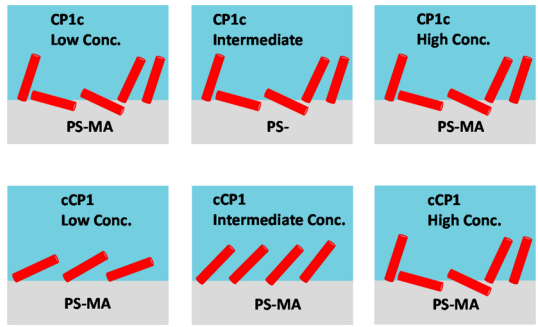

Figure 6. Schematics showing the different peptide concentration-dependent immobilization behaviors of CP1c and cCP1.

for such differences. This difference might be due to the differences in the peptide segments near the N-terminus and the C-terminus of CP1. The N-terminus of CP1 is amphiphilic and positively charged, while the C-terminus is hydrophobic. Our further experiments on chemically immobilized CP1c and cCP1 on maleimide-terminated self-assembled monolayers show that they behave very differently. Both SFG experimental studies and molecular dynamics simulations indicate such distinct differences on SAMs. In conjunction with structural studies of CP1 immobilized on SAMs, investigation of the binding of bacterial lipolysaccharides to both CP1c and cCP1 have shown the effect of immobilization not just on peptide orientation but on interaction with analyte molecules.[17] For the polymer system studied here, more details about the different molecular interactions between PS-MA and cCP1 and CP1c are being investigated using molecular dynamics simulations and will be reported in the future.

4. CONCLUSION

In this research, SFG spectra were collected from cCP1 molecules at the PS-MA/peptide buffer solution interface of different peptide solution concentrations using different polarization combinations ssp and ppp. All detected SFG spectra are dominated by a single peak centered at ~1650 cm^{-1}, showing that cCP1 molecules adopted an α-helical conformation at the PS-MA/peptide solution interface, which is similar to previous results from the CP1c molecules. In previous studies, the χ_{ppp}/χ_{ssp} signal strength ratio of CP1c molecules collected from the PS-MA/peptide solution was found to be independent of the peptide solution concentration. The χ_{ppp}/χ_{ssp} ratio remains the same for CP1c concentrations varied from 0.56 to 75 μM in buffer, leading to a multiple-orientation distribution. However, for the cCP1 molecules, the χ_{ppp}/χ_{ssp} ratio changes as a function of the peptide concentration at lower peptide concentrations. cCP1 molecules at the PS-MA/peptide solution interface change orientation from more or less lying down at the interface at 0.19 μM to more or less standing up at the interface at 0.75 μM. When the peptide concentration becomes even higher, e.g., for 1.12, 1.50, and 3.74 μM, the cCP1 molecules at the interface adopt a multiple-orientation distribution because, in addition to the chemically immobilized cCP1 molecules, more physisorbed cCP1 molecules are found at the interface. The orientation angles of cCP1 at the PS-MA/peptide solution interface at different peptides concentration are summarized in Table 1.

We believe that this is the first observation of the different interfacial behavior of the same peptide immobilized on a surface via different termini using SFG. Such differences are

likely due to the different interfacial interactions. We also observed such differences using SFG on a simpler system in which peptides are immobilized on SAMs, and the results can be understood by molecular dynamics simulations, which will be reported in the near future. However, polymers are more widely applicable on various substrates than SAMs; therefore, further studies on interactions between peptides and PS-MA are being carried out using molecular dynamics and will be reported in the future. As we indicated previously, peptides have the potential to supplement antibodies for many biosensing applications. However, before peptide-based applications, such as sensors, can be developed, it is crucial to understand the peptide interfacial molecular structure in order to ascertain the potential effects on the desired analyte interactions. Our observations here that the same peptide immobilized at opposing termini take on different surface orientations is a key first step.

AUTHOR INFORMATION

Corresponding Author

*E-mail: Charlene.Mello@us.army.mil, zhanc@umich.edu.

Notes

The authors declare no competing financial interest.

ACKNOWLEDGMENTS

This research was supported by the Army Research Office (W911NF-11-1-0251).

REFERENCES

(1) Ivnitski, D.; Abdel-Hamid, I.; Atanasov, P.; Wilkins, E. Biosensors for detection of pathogenic bacteria. *Biosens. Bioelectron.* **1999**, *14* (7), 599−624.

(2) Lazcka, O.; Campo, F.; Muñoz, F. X. Pathogen detection: A perspective of traditional methods and biosensors. *Biosens. Bioelectron.* **2007**, *22* (7), 1205−1217.

(3) Leonard, P.; Hearty, S.; Brennan, J.; Dunne, L.; Quinn, J.; Chakraborty, T.; O' Kennedy, R. Advances in biosensors for detection of pathogens in food and water. *Enzyme Microb. Technol.* **2003**, *32* (1), 3−13.

(4) Zaytseva, N. V.; Goral, V. N.; Montagna, R. A.; Baeumner, A. J. Development of a microfluidic biosensor module for pathogen detection. *Lab Chip* **2005**, *5* (8), 805−811.

(5) Velusamy, V.; Arshak, K.; Korostynska, O.; Oliwa, K.; Adley, C. An overview of foodborne pathogen detection: In the perspective of biosensors. *Biotechnol. Adv.* **2010**, *28* (2), 232−254.

(6) Wang, J.; Rivas, G.; Cai, X. Screen-printed electrochemical hybridization biosensor for the detection of DNA sequences from the Escherichia coli pathogen. *Electroanalysis* **2005**, *9* (5), 395−398.

(7) Wang, J.; Rivas, G.; Cai, X.; Palecek, E.; Nielsen, P.; Shiraishi, H.; Dontha, N.; Luo, D.; Parrado, C.; Chicharro, M. DNA electrochemical biosensors for environmental monitoring. A review. *Anal. Chim. Acta* **1997**, *347* (1), 1−8.

(8) Song, J.; Cheng, Q.; Zhu, S.; Stevens, R. C. "Smart" Materials for Biosensing Devices: Cell-Mimicking Supramolecular Assemblies and Colorimetric Detection of Pathogenic Agents. *Biomed. Microdevices* **2002**, *4* (3), 213−221.

(9) Ecker, D. J.; Drader, J. J.; Gutierrez, J.; Gutierrez, A.; Hannis, J. C.; Schink, A.; Sampath, R.; Blyn, L. B.; Eshoo, M. W.; Hall, T. A. The Ibis T5000 universal biosensor: an automated platform for pathogen identification and strain typing. *J. Assoc. Lab. Autom.* **2006**, *11* (6), 341−351.

(10) Gregory, K.; Mello, C. M. Immobilization of Escherichia coli cells by use of the antimicrobial peptide cecropin P1. *Appl. Environ. Microbiol.* **2005**, *71* (3), 1130−1134.

(11) Arcidiacono, S.; Pivarnik, P.; Mello, C. M.; Senecal, A. Cy5 labeled antimicrobial peptides for enhanced detection of *Escherichia coli* O157:H7. *Biosens. Bioelectron.* **2008**, *23* (11), 1721−1727.

(12) Mello, C. M.; Soares, J. *Membrane selectivity of antimicrobial peptides*; ACS Symposium Series; ACS Publications: Washington, DC, 2007.

(13) Soares, J. W.; Kirby, R.; Morin, K. M.; Mello, C. M. Antimicrobial peptide preferential binding of E. Coli o157: H7. *Protein Pept. Lett.* **2008**, *15* (10), 1086−1093.

(14) Kulagina, N. V.; Lassman, M. E.; Ligler, F. S.; Taitt, C. R. Antimicrobial peptides for detection of bacteria in biosensor assays. *Anal. Chem.* **2005**, *77* (19), 6504−6508.

(15) Kulagina, N. V.; Anderson, G. P.; Ligler, F. S.; Shaffer, K. M.; Taitt, C. R. Antimicrobial peptides: New recognition molecules for detecting botulinum toxins. *Sensors* **2007**, *7* (11), 2808−2824.

(16) Kulagina, N. V.; Shaffer, K. M.; Anderson, G. P.; Ligler, F. S.; Taitt, C. R. Antimicrobial peptide-based array for *Escherichia coli* and *Salmonella* screening. *Anal. Chim. Acta* **2006**, *575* (1), 9−15.

(17) Uzarski, J. R.; Mello, C. M. Detection and classification of related lipopolysaccharides via a small array of immobilized antimicrobial peptides. *Anal. Chem.* **2012**, *84* (17), 7359−7366.

(18) Williams, R. A.; Blanch, H. W. Covalent immobilization of protein monolayers for biosensor applications. *Biosens. Bioelectron.* **1994**, *9* (2), 159−167.

(19) Banerjee, P.; Lenz, D.; Robinson, J. P.; Rickus, J. L.; Bhunia, A. K. A novel and simple cell-based detection system with a collagen-encapsulated B-lymphocyte cell line as a biosensor for rapid detection of pathogens and toxins. *Lab. Invest.* **2007**, *88* (2), 196−206.

(20) Jonkheijm, P.; Weinrich, D.; Schröder, H.; Niemeyer, C. M.; Waldmann, H. Chemical strategies for generating protein biochips. *Angew. Chem., Int. Ed.* **2008**, *47* (50), 9618−9647.

(21) Köhn, M. Immobilization strategies for small molecule, peptide and protein microarrays. *J. Pept. Sci.* **2009**, *15* (6), 393−397.

(22) Rusmini, F.; Zhong, Z.; Feijen, J. Protein immobilization strategies for protein biochips. *Biomacromolecules* **2007**, *8* (6), 1775−1789.

(23) Wang, J.; Mark, A.; Chen, X.; Schmaier, A. H.; Waite, J. H.; Chen, Z. Detection of amide I signals of interfacial proteins in situ using SFG. *J. Am. Chem. Soc.* **2003**, *125* (33), 9914−9915.

(24) Fu, L.; Ma, G.; Yan, E. C. Y. *In situ*misfolding of human islet amyloid polypeptide at interfaces probed by vibrational sum frequency generation. *J. Am. Chem. Soc.* **2010**, *132* (15), 5405−5412.

(25) Fu, L.; Liu, J.; Yan, E. C. Y. Chiral sum frequency generation spectroscopy for characterizing protein secondary structures at interfaces. *J. Am. Chem. Soc.* **2011**, *133* (21), 8094−8097.

(26) Fu, L.; Xiao, D.; Wang, Z.; Batista, V. S.; Yan, E. C. Y. Chiral sum frequency generation for *in situ*probing proton exchange in antiparallel β-sheets at interfaces. *J. Am. Chem. Soc.* **2013**, *135* (9), 3592−3598.

(27) Weidner, T.; Breen, N. F.; Li, K.; Drobny, G. P.; Castner, D. G. Sum frequency generation and solid-state NMR study of the structure, orientation, and dynamics of polystyrene-adsorbed peptides. *Proc. Natl. Acad. Sci. U.S.A.* **2010**, *107* (30), 13288−13293.

(28) Engel, M. F. M.; vandenAkker, C. C.; Schleeger, M.; Velikov, K. P.; Koenderink, G. H.; Bonn, M. The polyphenol EGCG inhibits amyloid formation less efficiently at phospholipid interfaces than in bulk solution. *J. Am. Chem. Soc.* **2012**, *134* (36), 14781−14788.

(29) Weidner, T.; Apte, J. S.; Gamble, L. J.; Castner, D. G. Probing the orientation and conformation of α-helix and β-strand model peptides on self-assembled monolayers using sum frequency generation and NEXAFS spectroscopy. *Langmuir* **2010**, *26*, 3433−3440.

(30) York, R. L.; Browne, W. K.; Geissler, P. L.; Somorjai, G. A. Peptides adsorbed on hydrophobic surfaces—asum frequency generation vibrational spectroscopy and modeling study. *Isr. J. Chem.* **2007**, *47* (1), 51−58.

(31) Chen, X.; Wang, J.; Boughton, A. P.; Kristalyn, C. B.; Chen, Z. Multiple orientation of melittin inside a single lipid bilayer determined

by combined vibrational spectroscopic studies. *J. Am. Chem. Soc.* **2007**, *129* (5), 1420−1427.
(32) Nguyen, K. T.; Le Clair, S. V.; Ye, S.; Chen, Z. Orientation determination of protein helical secondary structures using linear and nonlinear vibrational spectroscopy. *J. Phys. Chem. B* **2009**, *113* (36), 12169−12180.
(33) Nguyen, K. T.; King, J. T.; Chen, Z. Orientation determination of interfacial β-sheet structures in situ. *J. Phys. Chem. B* **2010**, *114* (25), 8291−8300.
(34) Li, H.; Ye, S.; Wei, F.; Ma, S.; Luo, Y. In situ molecular-level insights into the interfacial structure changes of membrane-associated prion protein fragment [118−135] investigated by sum frequency generation vibrational spectroscopy. *Langmuir* **2012**, *28*, 16979−16988.
(35) Ye, S.; Nguyen, K. T.; Boughton, A. P.; Mello, C. M.; Chen, Z. Orientation difference of chemically immobilized and physically adsorbed biological molecules on polymers detected at the solid/liquid interfaces in situ. *Langmuir* **2010**, *26* (9), 6471−6477.
(36) Mermut, O.; Phillips, D. C.; York, R. L.; McCrea, K. R.; Ward, R. S.; Somorjai, G. *In Situ*adsorption studies of a 14-amino acid Leucine-Lysine peptide onto hydrophobic polystyrene and hydrophilic silica surfaces using quartz crystal microbalance, atomic force microscopy, and sum frequency generation vibrational spectroscopy. *J. Am. Chem. Soc.* **2006**, *128* (11), 3598−3607.
(37) Yang, P.; Ramamoorthy, A.; Chen, Z. Membrane orientation of MSI-78 measured by sum frequency generation vibrational spectroscopy. *Langmuir* **2011**, *27* (12), 7760−7767.
(38) Han, X.; Soblosky, L.; Slutsky, M.; Mello, C. M.; Chen, Z. Solvent effect and time-dependent behavior of C-terminus-Cysteine-modified Cecropin P1 chemically immobilized on a polymer surface. *Langmuir* **2011**, *27* (11), 7042−7051.
(39) Boughton, A. P.; Yang, P.; Tesmer, V. M.; Ding, B.; Tesmer, J. J. G.; Chen, Z. Heterotrimeric G protein $\beta 1\gamma 2$ subunits change orientation upon complex formation with G protein-coupled receptor kinase 2 (GRK2) on a model membrane. *Proc. Natl. Acad. Sci.* **2012**, *108* (37), E667−E673.
(40) Ye, S.; Li, H.; Wei, F.; Jasensky, J.; Boughton, A. P.; Yang, P.; Chen, Z. Observing a model ion channel gating action in model cell membranes in real time in situ: membrane potential change induced Alamethicin orientation change. *J. Am. Chem. Soc.* **2012**, *134* (14), 6237−6243.
(41) Belkin, M. A.; Shen, Y. R. Non-linear optical spectroscopy as a novel probe for molecular chirality. *Int. Rev. Phys. Chem.* **2005**, *24* (2), 257−299.
(42) Shen, Y. R. *The principles of nonlinear optics*; Wiley-Interscience: New York, 1984; Vol. *575*, p 1.
(43) Shen, Y. R. Surface properties probed by second-harmonic and sum-frequency generation. *Nature* **1989**, *337*, 519−525.
(44) Williams, C. T.; Beattie, D. A. Probing buried interfaces with non-linear optical spectroscopy. *Surf. Sci.* **2002**, *500* (1), 545−576.
(45) Zhuang, X.; Miranda, P. B.; Kim, D.; Shen, Y. R. Mapping molecular orientation and conformation at interfaces by surface nonlinear optics. *Phys. Rev. B* **1999**, *59* (19), 12632.
(46) Lambert, A. G.; Davies, P. B.; Neivandt, D. J. Implementing the theory of sum frequency generation vibrational spectroscopy: A tutorial review. *Appl. Spectrosc. Rev.* **2005**, *40* (2), 103−145.
(47) Perry, A.; Neipert, C.; Space, B. Theoretical modeling of interface specific vibrational spectroscopy: methods and applications to aqueous interfaces. *Chem. Rev.* **2006**, *106* (4), 1234−1258.
(48) Leung, B. O.; Yang, Z.; Wu, S. S. H.; Chou, K. C. Role of interfacial water on protein adsorption at cross-linked polyethylene oxide interfaces. *Langmuir* **2012**, *28* (13), 5724−5728.
(49) Chen, P.; Kung, K. Y.; Shen, Y. R.; Somorjai, G. A. Sum frequency generation spectroscopic study of CO/Ethylene coadsorption on the Pt(111) surface and CO poisoning of catalytic Ethylene hydrogenation. *Surf. Sci.* **2001**, *494* (3), 289−297.
(50) Tong, Y.; Tyrode, E.; Osawa, M.; Yoshida, N.; Watanabe, T.; Nakajima, A.; Ye, S. Preferential adsorption of amino-terminated silane in a binary mixed self-assembled monolayer. *Langmuir* **2011**, *27* (9), 5420−5426.
(51) Ye, H. K.; Gu, Z. Y.; Gracias, D. H. Kinetics of ultraviolet and plasma surface modification of poly(dimethylsiloxane) probed by sumfrequency vibrational spectroscopy. *Langmuir* **2006**, *22* (4), 1863−1868.
(52) Kim, J.; Cremer, P. S. IR-Visible SFG investigations of interfacial water structure upon polyelectrolyte adsorption at the solid/liquid interface. *J. Am. Chem. Soc.* **2000**, *122* (49), 12371−12372.
(53) Bordenyuk, A. N.; Jayathilake, H.; Benderskii, A. V. Coherent vibrational quantum beats as a probe of Langmuir-Blodgettmonolayers. *J. Phys. Chem. B* **2005**, *109* (33), 15941−15949.
(54) Baldelli, S. Surface structure at the ionic liquid-electrified metal interface. *Acc. Chem. Res.* **2008**, *41* (3), 421−431.
(55) Davis, A. P.; Ma, G.; Allen, H. C. Surface vibrational sum frequency and Raman studies of PAMAM G0, G1 and acylated PAMAM G0 dendrimers. *Anal. Chim. Acta* **2003**, *496* (1−2), 117−131.
(56) Voges, A. B.; Al-Abadleh, H. A.; Musorrariti, M. J.; Bertin, P. A.; Nguyen, S. T.; Geiger, F. M. Carboxylic acid- and ester-functionalized siloxane scaffolds on glass studied by broadband sum frequency generation. *J. Phys. Chem. B* **2004**, *108* (48), 18675−18682.
(57) Can, S. Z.; Mago, D. D.; Walker, R. A. Structure and organization of hexadecanol isomers adsorbed to the air/water interface. *Langmuir* **2006**, *22* (19), 8043−8049.
(58) Liu, J.; Conboy, J. C. Direct measurement of the transbilayer movement of phospholipids by sum-frequency vibrational spectroscopy. *J. Am. Chem. Soc.* **2004**, *126* (27), 8376−8377.
(59) Rao, Y.; Comstock, M.; Eisenthal, K. B. Absolute orientation of molecules at interfaces. *J. Phys. Chem. B* **2006**, *110* (4), 1727−1732.